

Crystallization of Janus-Wedge Triplexes by Hanging Drop Vapor Diffusion

Author: Michael Joseph Hemak

Persistent link: <http://hdl.handle.net/2345/360>

This work is posted on [eScholarship@BC](#),
Boston College University Libraries.

Boston College Electronic Thesis or Dissertation, 2005

Copyright is held by the author, with all rights reserved, unless otherwise noted.

Crystallization of Janus-Wedge Triplexes by Hanging Drop Vapor Diffusion

Senior Honors Thesis
Michael J. Hemak
Advisor: Larry McLaughlin
Boston College Biochemistry Department
2004-2005

Abstract

The ability to control gene expression has traditionally been pursued at the protein level, using drugs designed to mimic a natural substrate or to disrupt a protein's active site. Traditional drug targeting by competitive and non-competitive inhibitors, however, requires a fairly detailed knowledge of the target protein's three-dimensional structure. More recently, focus has broadened to include alternative methods of genetic control, including the use of single-stranded DNA or RNA probe sequences which control gene expression by targeting the genes themselves. Within the last two decades, peptide nucleic acids (PNAs) – DNA mimics possessing natural bases linked to an N-(2-aminoethyl)-glycine (AEG) backbone – have proven as effective in gene-targeting as traditional synthetic DNA or RNA with the added advantages of tighter binding and greater specificity. Additionally, PNAs are not easily recognized by nucleases, proteases, and peptidases giving them greater resistance to enzyme degradation and making them even more favorable for gene targeting *in vivo*.

Traditional PNA triplexes are composed of two polypyrimidine PNA strands bound to the Watson-Crick and Hoogsteen faces, respectively, of the polypurine strand of target DNA after displacing the polypyrimidine strand of the original DNA duplex. Janus Wedge (JW) residues, on the other hand, utilize unnatural bases linked to the AEG backbone, which are capable of hydrogen bonding to the Watson-Crick faces of both strands of a target DNA duplex. JW triplex formation, then, has a DNA₂-PNA stoichiometry, and no Hoogsteen face interactions.

The generalization of the DNA duplex targeting strategy by peptide oligomers requires substantial discoveries in the field of PNA research, including an understanding

of the three-dimensional structure and folding pattern of these triple-stranded molecules. This report details the crystallization efforts on JW DNA-peptide-DNA triplexes using 11dC₈11-11T₈11 target sequences – with and without single base overhangs – and synthetic W₈K peptide. Hanging drop vapor diffusion methods showed that while crystal formation was extremely elusive, in narrowing the optimal buffer conditions, 25% PEG concentration was consistently correlated with the most promising crystallization efforts for both the overhanged and non-overhanged sequences.

Introduction

The field of triple stranded DNA research traces its lineage back to Felsenfeld *et al.* who is believed to have made the first discovery of a triple stranded molecule in 1957.¹ While studying the complexing reaction of synthetic polyadenylic acid (poly-A) and polyuridylic acid (poly-U) in aqueous solution, a complex was discovered with a sedimentation coefficient significantly greater than the 1:1 duplex. Subsequent analysis of this new complex revealed that its formation was optimized by a U₂:Abase ratio in solution, suggesting a poly(U-A-U) triplex, which Felsenfeld postulated was the result of binding of a single poly(U) strand to a poly(A-U) duplex in the helical groove. He proposed that additional hydrogen bonds with one or both members of the Watson-Crick (W-C) duplex provided stability for the three-stranded molecule.

The next major breakthrough in the field of DNA triplexes came over two decades later when Lee *et al.* expanded on their previous finding that cytosine could form a triple stranded complex with a cytosine-guanine duplex only if it was protonated – a requirement which restricts C⁺-G-C formation to pHs below 6.² The modified residue 5-methylcytosine (m⁵C), however, could form a stable m⁵C-G-C triplex at neutral pH (pH

8.0).³ Based on these findings, Lee proposed methylation of cytosine as one method of controlling triplex stability. Both C^+-G-C and m^5C-G-C triplexes form from the binding of an additional polypyrimidine (py) strand to the polypurine (pu) strand of a polypurine•polypyrimidine duplex – a finding consistent with Felsenfeld's research.

The preference for py-pu-py triplex formation rather than pu-py pu stems from the chemical properties of the central nucleotide. While participating in W-C base pairing, purines have a second binding face, known as the Hoogsteen face, exposed for additional hydrogen bonding interactions with a second pyrimidine base (Figure 1).

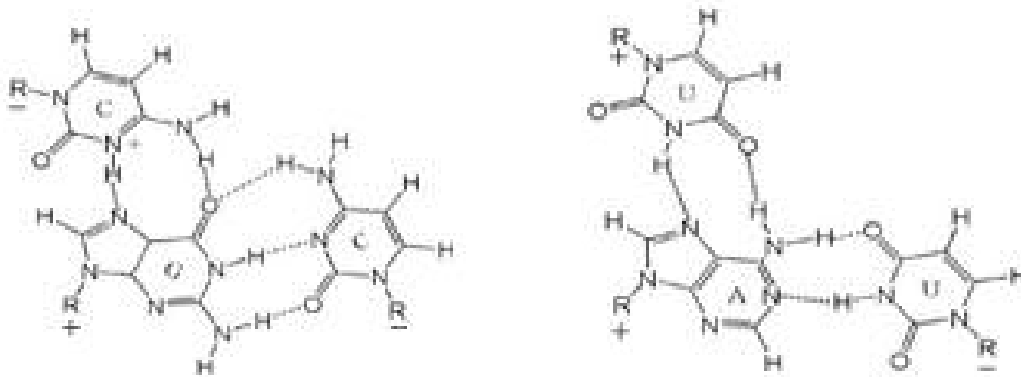


Figure 1: Hydrogen Bonding at Watson-Crick and Hoogsteen faces of C^+-G-C and $U-A-U$ Triplexes⁴

When DNA duplexes fold into their traditional B-form helices, the Hoogsteen face of purines is accessible in the major groove. This conformation suggests a mechanism for interaction between the polypurine of duplex DNA and a polypyrimidine⁵ (i.e. T-A-T) or polypurine⁶ (i.e. A-A-T) probe strand, with the polypurine strand forming a second set of hydrogen bonds with the single strand entering in the major groove. Pyrimidines, however, lack a Hoogsteen face, preventing the formation of similar bidentate interactions, and explaining the preference for py-pu-py, rather than pu-py pu, triplexes. The obvious downside of these types of triplexes is that they are limited to polypurine

targets, which stands as a significant obstacle to the generalized recognition motif necessary for eventual application to natural, rather than synthetic, DNA target sequences.

In addition to natural and modified DNA oligonucleotides, it was discovered that third strand binding could be accomplished by DNA mimics, known as peptide nucleic acids (PNAs). Structurally, PNAs possess a backbone consisting of repeating AEG monomers linked by peptide bonds (Figure 2). Like DNA, PNAs use natural purine and pyrimidine bases (A, T, C, and G) linked to the peptide backbone by methylene carbonyl bonds. However, unlike DNA, PNAs lack any pentose sugars and phosphate groups making them more resistant to DNA degradation enzymes such as nucleases and proteases.

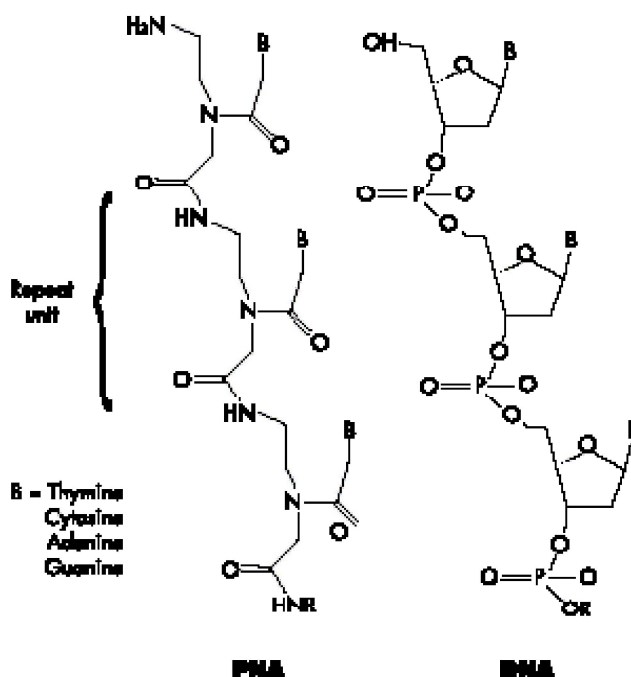


Figure 2: Structural Comparison of DNA and PNA Backbone⁷

PNAs are also stable over a large pH range, and the neutrality of their peptide backbone minimizes charge-charge repulsion interactions with DNA phosphate groups. For all these reasons, PNAs have emerged as a desirable alternative to DNA and RNA for studies of triple helix formation.

PNA triplexes form by a strand invasion mechanism beginning with the displacement of the polypyrimidine strand of a DNA duplex target by a polypyrimidine PNA probe strand. Watson-Crick hydrogen bonds between the bases of the PNA and polypurine strand stabilizing the formation of a PNA/DNA double helix. When folded, the Hoogsteen face of the polypurine strand lies exposed in the major groove, to which a second polypyrimidine PNA strand binds to complete the PNA DNA-PNA triplex, while the displaced polypyrimidine DNA strand remains in the characteristic D-loop conformation (Figure 3).

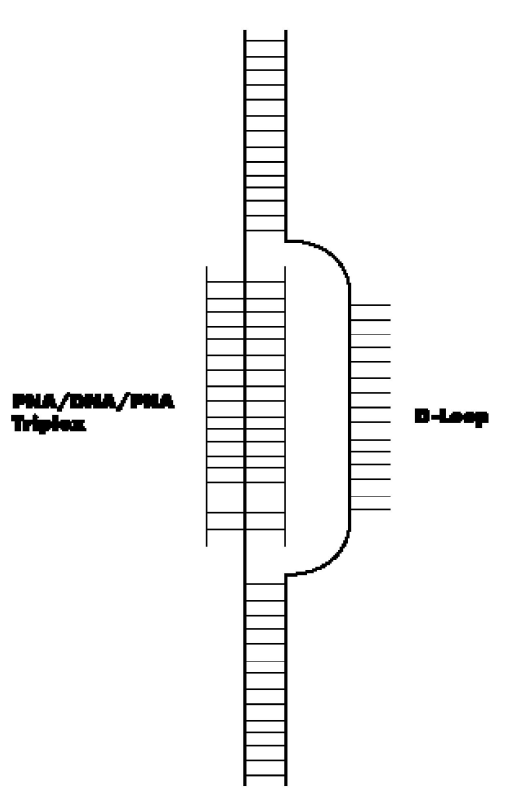


Figure 3: Strand Invasion by a PNA to Form PNA-DNA PNA Triplex and D-Loop⁸

Bearing some similarities to traditional PNAs, Janus Wedge (JW) triplexes – a formation first suggested by Lehn in his work with heterocycles⁹ – represent a fundamentally new approach to duplex DNA targeting. JW residues are structurally composed of an AEG peptide backbone linked by methylene carbonyl bonds to their respective bases. Unlike traditional PNAs which utilized the natural A, G, T, and C bases, JW residues contain unnatural bases chemically synthesized to be able to hydrogen bond with the Watson-Crick faces of two different natural bases (see Figure 4). Appropriately, JW triplexes are named for the Roman god Janus, who is traditionally depicted with two faces – one looking ahead at the future and one looking behind at the past.

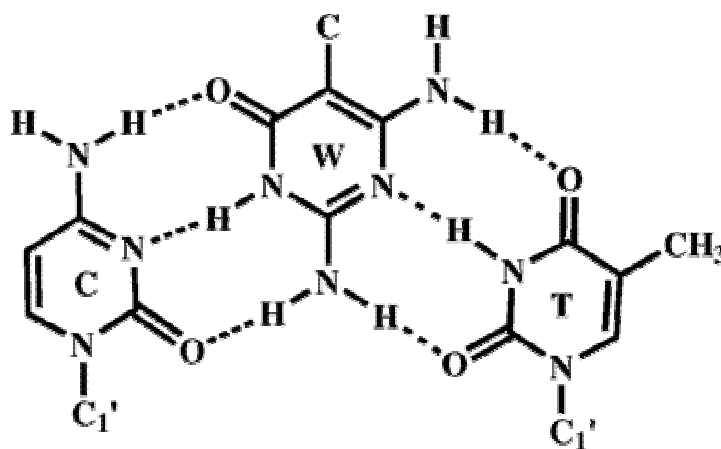


Figure 4: Hydrogen Bond Interactions of DNA-PNA-DNA Triplex at Watson-Crick Faces of DNA Bases¹⁰

The seemingly minor change from natural to unnatural bases in JW residues results in an entirely novel triplex and mechanism of formation. Unlike PNAs which bind to the polypurine of duplex DNA and displace the polypyrimidine during strand invasion, JW residues form hydrogen bonds with the W-C faces of both strands of the target DNA following insertion into the duplex. As a result of this increased number of hydrogen bonds, JW triplexes are proposed to be more stable relative to the DNA duplex. Unlike

traditional PNAs which are PNA-DNA-PNA triplexes, JW triplexes bind with DNA₂:PNA stoichiometry. Finally, JW triplexes are distinguished from traditional PNA triplexes in that no Hoogsteen face is involved in the final triple-stranded complex

Previous research conducted by Chen *et al.* under the supervision of Larry McLaughlin has elucidated several important characteristics of JW triplexes on which this research builds.¹¹ Their work focused on a 30-nucleotide synthetic duplex containing a non-complementary (C₈-T₈) target sequence flanked by eleven complementary W-C base pairs (Figure 5, next page). The non-complementary target ensured JW triplex formation did not need to compete with the duplex form, which would occur for complementary targets. The JW peptide probe was synthesized from eight repeating N⁶-amino-pseudocytidine (W) residues linked to an L-lysine (K) residue, and attached to an AEG backbone. They showed that the W₈K oligomer binds to both DNA strands individually by gel shift assay, but could not confirm the nature of the binding. Their work also suggested that, similar to traditional PNA triplexes, JW insertion occurs in the major groove of the target duplex. Also, thermodynamic studies confirmed that triplex formation occurs with binding to both strands of the DNA duplex, and revealed that the JW triplex is more stable than DNA-DNA-DNA or hairpin triplexes.



Figure 5: 11dC₈11-11dT₈11 DNA Duplex Target Sequence¹²

In light of their potential as gene-targeted drugs, the conformation and folding of DNA-, RNA-, and PNA-containing triplexes are of growing importance to researchers. In 1997, Rasmussen *et al.* successfully crystallized two self-complementary PNAs, H-CGTACG-NH₂ and H-CGBrUACG-NH₂, using the hanging drop vapor diffusion method (see “Materials and Methods” section for detail).¹³ Crystals were diffracted to 1.7 Å resolution by x-ray crystallography. The PNA-PNA duplex was found to adopt a unique helical structure stabilized by eighty-two water molecules forming bridges between purine-N3 or pyrimidine-O2 and backbone amide N at each base step. The structure was believed to support the belief that the natural bases prefer stacking in A-like helices. Mismatch analysis confirmed W-C base pairing rules were followed throughout the helix. The hanging drop vapor diffusion method was also employed by Kastrup *et al.* to crystallize a DNA-PNA duplex at about 5 Å resolution.¹⁴ When compared to the typical B-form DNA duplex, their experiments revealed that PNA is almost a perfect structural mimic of DNA. The DNA-PNA helix is structurally similar to a B-form helix, and like the PNA-PNA self-complementary duplex, it was found to obey the W-C base pairing rules throughout the helix.

Crystallization efforts on peptide nucleic acid triplexes have been focused primarily on traditional PNA-DNA-PNA triplexes. Bettset *al.*, for example, successfully crystallized a triplex consisting of a polypurine DNA strand complexed to a polypyrimidine hairpin PNA¹⁵. Conformationally, the triplex was found to be unique among previously known nucleic acid structures, and was designated as P-form, thereby expanding the number of stable helical forms which nucleic acids may adopt. Despite the progress made in crystallizing traditional PNA triplexes, Janus Wedge triplexes have

proven much more difficult to crystallize and x-ray analysis of JW triplexes is not well documented. Considering the potential of PNAs for transcriptional control of gene expression coupled with the unique mechanism of insertion and triplex formation used by Janus Wedge PNAs, the pressure is on to obtain three-dimensional data of these DNA-PNA-DNA structures through x-ray crystallography.

Materials and Methods

Chemicals and Materials: The phosphoramidites and reagents for DNA synthesis were purchased from Glen Research. Polyethylene glycol (PEG) 4000, 6000, 8000, and 10000 were purchased from Fluka. Spermine and spermidine were purchased from Sigma-Aldrich. Crystallization plates and siliconized coverslips were purchased from Hampton Research. 0.22 μm centrifugal filtration devices were purchased from Millipore. Spermine Tetrahydrochloride was purchased from United States Biochemical (USB). 2-methyl-2,4-pentanediol (MPD) was purchased from Sigma-Aldrich. Synthesized and purified M1-219 JW peptide was obtained from post-doctorate researcher Meena. 2-amino-pyrimidine substituted Dickerson dodecamer DNA was obtained from post-graduate researcher Zhenhua.

DNA Synthesis: Single strand DNA sequences were synthesized using an Applied Biosystems 394 DNA/RNA Synthesizer from standard dNTP monomers (sequences listed in Appendix C). Syntheses were carried out on a 1.0 μmol scale with 30-35 mg of the 3' terminal dNTP added as starting material to the column. Chemically, these 3' terminal monomers were bound to a controlled pore glass (CPG) solid support at the 3' position, and blocked with a dimethoxytrityl (DMT) group at the 5' position. Synthesis

proceeded with 3' → 5' directionality following the generalized assembly pathway depicted in Appendix A¹⁶, with capping of unreacted dNTPs after each coupling step. Final sequence purity was consistently over 98% (measured relative to the amount of reacted sequence after the first coupling).

DNA Isolation and Purification: The synthesized DNA oligomers were first dried under line vacuum for 3-5 minutes and transferred to eppendorf tubes. ~2 mL of concentrated ammonium hydroxide (NH₄OH) were added to each tube, which were then placed in a 55°C water bath for 8-10 hours. Ammonium hydroxide treatment accomplishes three tasks: 1.) strand cleavage from CPG support, 2.) removal of exocyclic amine protecting groups on C, G, and A bases, and 3.) removal of cyanoethoxy protecting groups on the backbone phosphates. Passing the solutions through cotton-plugged glass pipettes filtered out the CPG, and then the volumes were reduced under high vacuum to < 1 mL. The oligomers were syringe-filtered (0.22 µm) using several mL of dH₂O as wash. Purification was begun by high performance liquid chromatography (HPLC) using a Semi Prep C18 (OliR3) reversed phase column measuring absorbance at 254.0 nm. Prior to connecting the HPLC lines, Buffer A (50 mM TEA) and Buffer B (50 mM TEA, 70% acetonitrile) were vacuum filtered through a Millipore 0.45 micron HA filter to remove microparticles and degas the solutions. The HPLC cycle alternated between a 5 minute column conditioning (POROSHQ20Wash) and a 12 minute injection (oliR3). Next, detritylation (removal of DMT group) was achieved by addition of ~2 mL of 80% acetic acid in H₂O to the oligomers, which were placed on ice for 20 minutes. The acetic acid was evaporated, followed by 2-3 co-evaporations with 10 mL of ethanol, under high vacuum using a rotary evaporator (rotovap). Detritylated oligomers were desalted using a

Sephadex G-10 column, flash frozen by immersion in liquid N₂, and finally lyophilized overnight. Sample concentration was determined by UV spectroscopy at 254.0 nm. 5 µL of the DNA oligomer were diluted to 1.0 mL with dH₂O, representing a 200-fold dilution, prior to spectrophotometer detection, and the sample concentration was calculated by the equation:

$$200 * \text{Absorbance} = \text{extinction coefficient} * \text{path length} * \text{concentration}$$

A table of pertinent extinction coefficients is included as Appendix B.

Peptide Synthesis¹⁷: Cbz protected 2,4-diamino 6-oxo pyrimidine monomer (Figure 6) having an ethylene glycol backbone was synthesized in six steps and was characterized by NMR (Nuclear Magnetic Resonance) and HRMS (High Resolution Mass Spectrometry). Sequential assembly of L-Lys and JW monomers on MBHA (4-Methylbenzhydryl Amine) resin using standard peptide coupling protocol provided the protected oligomer, which was cleaved from the support using the TFMSA cleavage

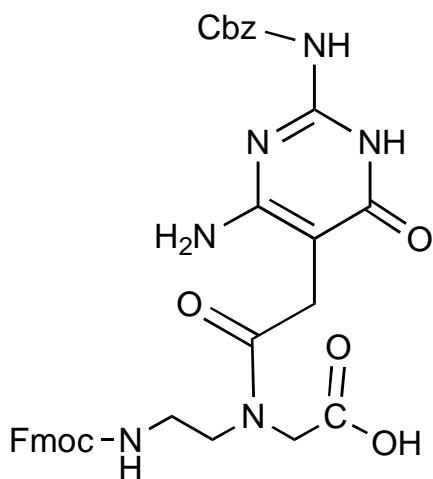


Figure 6: Peptide Synthesis Starting Material: Cbz-protected 2,4-diamino-6-oxo-pyrimidine

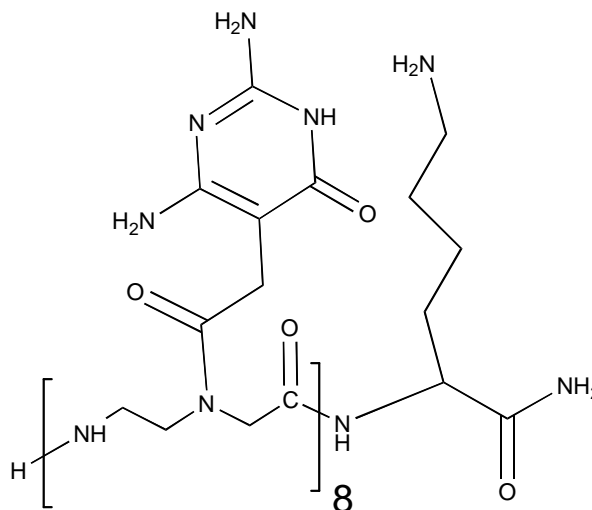


Figure 7: Structure of Peptide Nucleic Acid M1-219

method to obtain free peptide nucleic acid, M1-219 (Figure 7, previous page). The peptide was purified by HPLC using a Semi Prep C18 reversed phase column and was characterized by MALDI TOF. The calculated mass for $C_{18}H_{127}N_{51}O_{25}$ was determined to be 2275.2 Da, and the observed mass was 2275.2 Da.

Gel Electrophoresis: The synthesized DNA was annealed and checked by gel electrophoresis for proper duplex and/or triplex formation. After calculating the amount of DNA or peptide needed for a gel or crystallization plate, these volumes were aliquoted into eppendorf tubes and dried under high vacuum in a Jouan RC 10.22 speedvac. Dried samples were resuspended with the appropriate volume of annealing buffer, and added to a beaker containing ~1000 mL of 90-100°C water. After cooling to room temperature, the beaker and samples were transferred to a 4°C environment. Samples were run on a 20% (19:1 acrylimide:bis-acrylimide) non-denaturing gel washed for 30 minutes at 150 V (constant voltage) with 1X TBE (Tris-Borate-EDTA) buffer. The volume of DNA solution loaded into each lane was determined by standardizing to a 0.5 absorbance for the sample. Loading buffer containing 30% glycerol (otherwise identical to the annealing buffer) was added to each sample prior to loading on the gel. Gels were run at 250 V (constant voltage) for 15-17 hours with 1X TBE buffer. Gels were stained with ethidium bromide for 10 minutes and visualized using Bio-Rad Molecular Imager FX using an ethidium bromide filter. As a precaution, prior to crystallization work, triplex DNA was filtered through a 0.22 µm Ultrafree-MC centrifugal filter at 10,000 rpm to remove microparticles.

Hanging Drop Vapor Diffusion: Although there are several methods for crystallizing macromolecules, vapor diffusion methods, first used to crystallize tRNA,¹⁸

have emerged as one of the most popular and successful, particularly when working with small volumes. To make a plate, a reservoir solution is prepared containing buffer (sodium cacodylate, specific pH), crystallizing agent or precipitant (PEG), and additives (zinc acetate, magnesium acetate, ammonium acetate), and a small volume of this solution is mixed with a small volume of macromolecule-containing solution on a siliconized glass coverslip. This droplet is sealed by a ring of silicone grease over the reservoir, containing a higher concentration of precipitant, and the gradual equilibration of the two solutions promotes the crystallization process. Crystallization experiments were performed using 24-well Linbro boxes and 22 mm siliconized glass slides at 4°C.

Results and Discussion

JT Sequences: The JT sequences shown in Appendix C were designed to have a non-complementary T₈-C₈ target sequence flanked by complementary 11-base pair segments. The base composition and purity of the single strands was confirmed by gel electrophoresis (see Figure 4, next page). A 300 µM sample of single-stranded JT-2 and JT-3 was loaded into lanes 1 and 2, respectively, whose bands corresponded to low molecular weight, non-identical species. A single band corresponding to a higher molecular weight species in lane 3 containing both JT-2 and JT-3 confirms duplex formation occurs with a high degree of efficiency. Lane 5, containing JT-2, JT-3, and 1.0 equivalents of M1-219 peptide, shows a slight duplex band, and a second higher molecular weight species corresponding to DNA-PNA DNA triplex (lane 4 was blank). Single-stranded and duplex DNA were annealed with 10 mM HEPES, pH 7.0 with 50 mM NaCl and 10 mM MgCl₂. Triplex DNA was annealed with 10 mM HEPES, pH 7.0

and 1 mM spermidine – an additive used for its ability to stabilize the negative charges of the phosphate backbone.

The first crystallization plate was prepared from this 300 μ M sample of JT-2 + JT-3 + M1-219 peptide (JT-2+3+p) annealed with 10 mM HEPES, pH 7.0, 1.0 mM spermidine. The reservoir conditions of the 24 wells are included in Appendix D, with each well containing a unique combination of pH, PEG molecular weight, and PEG concentration. The reservoirs contained 1 mL of buffer each, and each droplet contained 1 μ L of triplex solution mixed with 1 μ L of reservoir buffer. Immediately after plating the samples, all wells appeared as clear drops under a microscope. After three days, precipitates had formed in all the wells except the four wells containing 30% PEG 8000, regardless of pH, which displayed a combination of precipitate and some microcrystals.

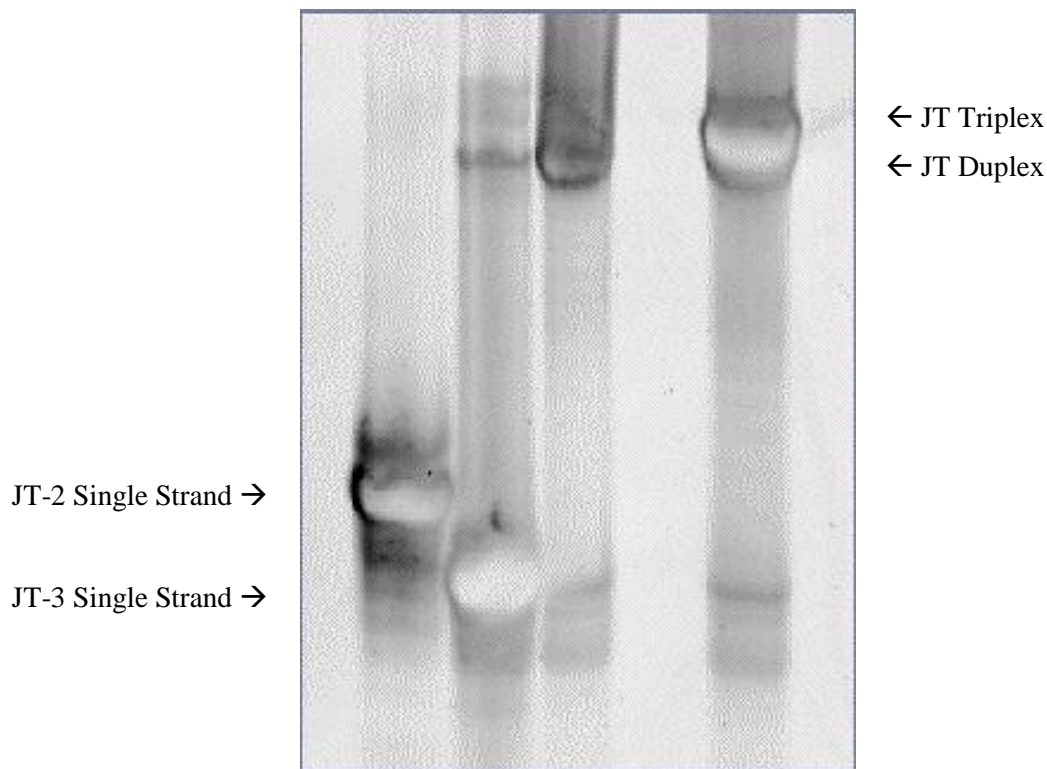


Figure 8: JT-2+3 Duplex (lane 3) and JT-2+3+p Triplex Formation (lane 5) at 300 μ M

The largest microcrystals were present in well 23, containing 30% PEG 8000, pH 7.5. These four wells showed no significant change up to one month after plate preparation, but after three months, the solution in well 23 had precipitated completely and microcrystals were no longer present, although the solutions in wells 5, 11, and 17 were unchanged.

This initial promise of PEG 8000 prompted the design of a second crystallization plate which focused exclusively on this molecular weight. However, as shown in Appendix E, the JT-2+3+p triplex concentration became one of the variables under investigation as samples of 200, 225, 250, and 300 μM were annealed (see Figure 9, next page). The intensity of the duplex band indicated the formation of a large amount of JT duplex despite the presence of peptide in solution. To promote triplex, rather than duplex, formation, 20% more peptide was added to each triplex sample, and as shown in Figure 10 (next page), the concentration of JT duplex decreased while the intensity of the JT triplex band increased as desired. The annealing buffer, temperature, drop volume, drop composition, and reservoir volume were held consistent with Plate 1. Interestingly, the 200 μM triplex precipitated immediately after plating, while the remaining three concentrations were clear droplets. After one week, precipitation was observed in all 24 wells, regardless of complex concentration, indicating that new adjustments to the crystallization variables must be tested.

The third crystallization plate tested the hypothesis that crystal formation was dependent upon the volume of buffer in the reservoir, the ratio between drop volume and reservoir volume, or both. Because lower sample concentrations proved unsuccessful in

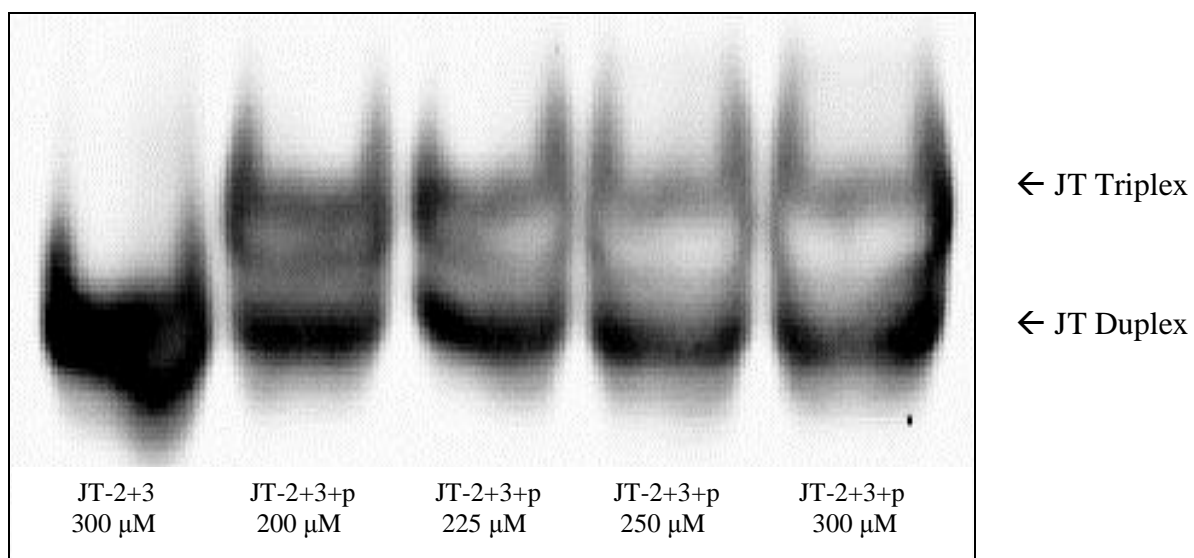


Figure 9: JT-2+3+p Triplex Formation with 1:1 PNA Equivalents

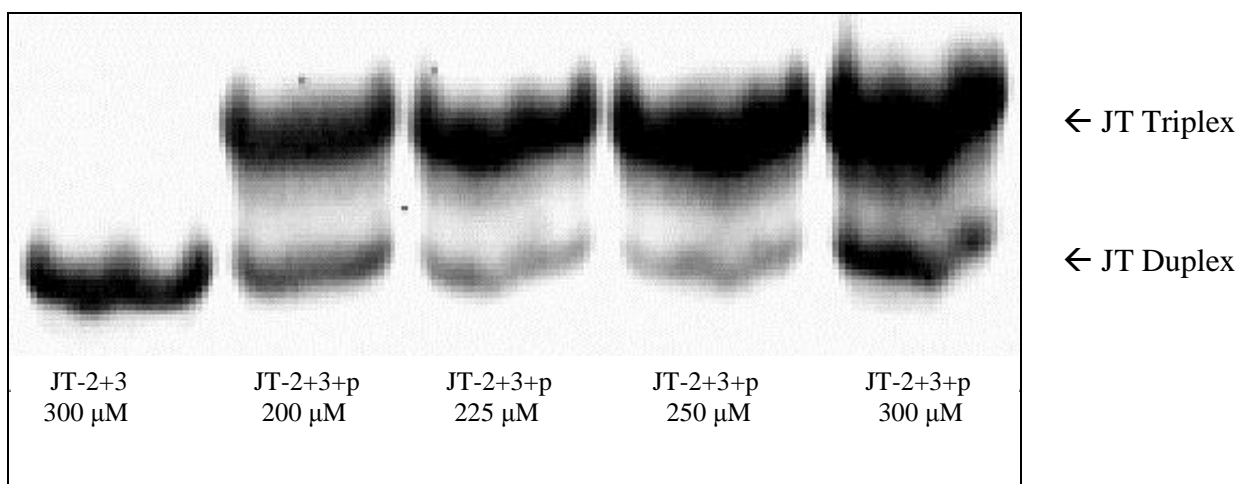


Figure 10: JT-2+3+p Triplex Formation with 1.2 PNA Equivalents

Plate 2, complex concentration was increased to 400 μ M hoping that a higher concentration would improve yield, and 1.7 PNA equivalents were used to anneal the triplex. As shown in Appendix F, the reservoirs contained either 1.0 mL or 0.5 mL with either a 1:1 or 2:1 ratio of sample to buffer in the droplet. The different reservoir buffers tested were specifically chosen from successful crystallization work previously done by

post-doctorate researcher Meena. In her work, magnesium acetate, rather than zinc acetate was used in the reservoir buffers, so this substitution was made accordingly in an attempt to replicate her results. Initially after plating, all 24 wells were clear drops, but within three days, only well 4 showed any possibility of microcrystal formation, and after 2.5 months, all wells had completely precipitated.

Crystallization Plate 4 continued to probe the effect of altering sample to buffer ratio and reservoir volume, while also investigating whether a higher molecular weight PEG as precipitant or crystallizing agent could more successfully promote JT-2+3+p crystal growth (Appendix G). Returning to 300 μ M triplex concentration annealed with 10 mM HEPES, pH 7.0, 1 mM spermidine and 1.5 PNA equivalents, Plate 4 studied both PEG 8000 and PEG 10000. After plating, all drops appeared clear under microscope indicating no immediate precipitation was occurring. After six days, the droplet of well 21 was characterized as a birefringent precipitate or microcrystals. Interestingly, well 21 contained 30% PEG 8000 at pH 6.5, which had previously shown encouraging results in the first crystallization plate studied. This well, however, differed in two respects from Plate 1: 1.) it contained magnesium acetate rather than zinc acetate as additive, and 2.) the total reservoir volume was 0.5 mL rather than 1.0 mL. After eight days, four new wells were generated from the original droplet in an effort to increase crystal size. 0.25 μ L of the original droplet was pipetted onto a new glass slide and mixed with 1.00 μ L of buffer identical to that contained in the reservoir of well 21. It was hoped that repeating the process of reaching droplet-buffer equilibrium would promote the crystallization of JT triplex still in solution onto the microcrystal (acting as a sort of template). However, of these four wells, all had precipitated within two weeks without showing any increase in microcrystal size.

Based on the findings from Plates 1 and 4, crystallization plate 5 was dedicated exclusively to 30% PEG 8000, varying the pH (6.0, 6.5, 7.0, and 7.5) as well as sample to buffer ratio (1:1, 2:1, and 2:2) (Appendix H). Using 300 μ M complex with 1.5 PNA equivalents, this plate showed complete precipitation after less than one week. Crystallization Plate 6 focused exclusively on the PEG 10000 at 4 different pHs and 4 different PEG percentages, and alternating between zinc acetate and magnesium acetate as additive (Appendix I). Precipitation occurred in all 24 wells after about two months of incubation at 4°C without observation of any potential crystal formation. Crystallization plate 7 focused on the two well conditions which had proven most successful during previous crystallization work by Meena in the hopes of duplicating or improving on her results (Appendix J). The first buffer duplicated in wells 1-12 of Plate 7 contained 0.01 M Mg acetate, 0.2 M ammonium acetate, 0.05 M Na cacodylate, pH 6.0, and 35% PEG 8000. The second buffer contained in wells 13-24 of Plate 7 was composed of 0.01 M Mg acetate, 0.2 M ammonium acetate, 0.05 M Na cacodylate, pH 6.5, and 25% PEG 4000. After almost two months, each of the PEG 8000 wells had precipitated, and the PEG 4000 wells are still clear with no crystal formation yet observed.

JW Sequences: As shown in Appendix C, the JW sequences were designed to have a non-complementary (C₈-T₈) target sequence flanked by 11 Watson-Crick base pairs similar to the JT sequences. However, the JW strands were distinguished by a single base overhang at the 5' terminus (either A or T). When annealed as duplex or triplex, these single base overhangs would remain exposed, with the hope that the thymine overhang of one duplex would form a W-C base pair with the adenine overhang of a second duplex – leaving an unpaired T and A still exposed at the 5' termini (Figure 11).

(5') T GCA CCG ACG CGT TTT TTT TCC GCG GCA GCC (3')
 (3') CGT GGC TGC GCC CCC CCC CGG CGC CGT CGG A CGT GGC TGC GCC CCC CCC CGG CGC CGT CGG A (5')

Figure 11: Laddering of JW Sequences (single JW duplex underlined)

This laddering effect was hoped to improve crystal formation by promoting the aggrandizing of the macromolecule. One complication resulting from these overhangs, however, was the ability to visualize the JW duplex and triplex as a single, distinct band by gel electrophoresis to ensure complex formation. As seen in Figure 12, the JW strands showed gel streaking, indicative of the multiple molecular weight species formed by this laddering capacity. However, because laddering was ultimately desirable for crystallization purposes, streaking of non-denaturing gels was considered a positive and bearable result.

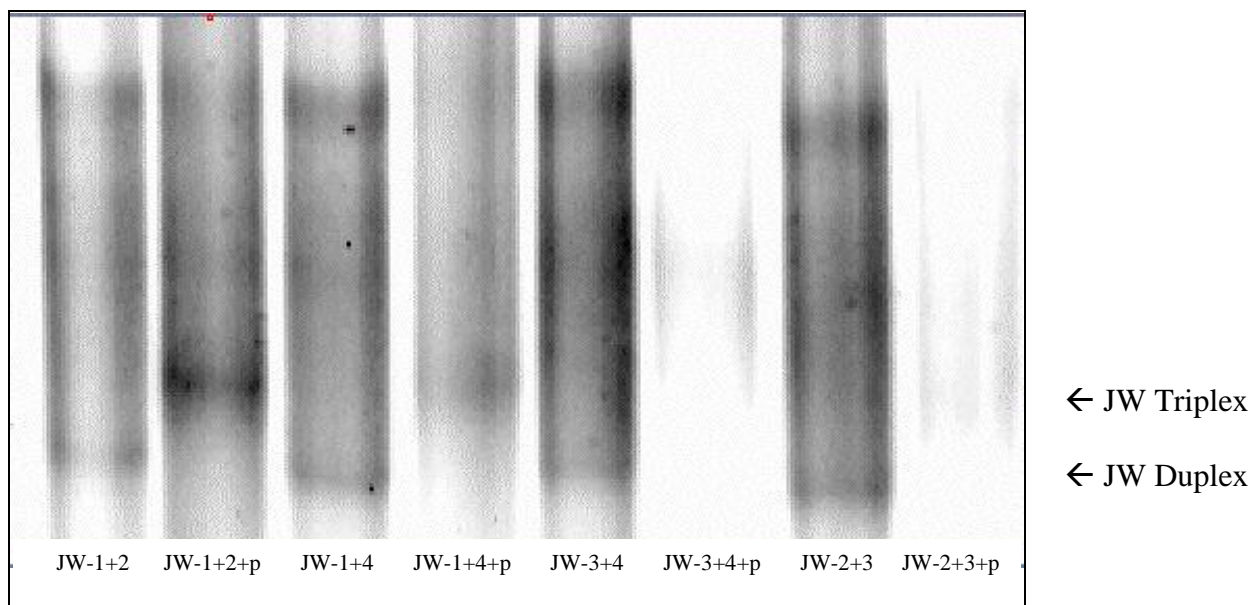


Figure 12: Duplex and Triplex Formation of JW Sequences at 300 μ M

Again, prior to any crystallization work, it was first necessary to confirm the base composition and purity of the synthesized JW strands by 20% non-denaturing gel (Figure 12, previous page). Lanes 2, 4, 6, and 8 contained annealed duplex, while lanes 3, 5, 7,

and 9 contained annealed triplex. Duplex formation was visualized in all four lanes, and a higher molecular weight species indicative of triplex formation was observed in lanes 3 and 5. The formation of very high molecular weight species in lanes 7 and 9, which subsequently could not migrate through the gel, may explain why these lanes appear washed out. JW duplexes were annealed with 25 mM HEPES, pH 7.0, 50 mM NaCl, 10 mM MgCl₂. JW triplexes were annealed with 25 mM HEPES, pH 7.0 (no spermidine).

40 μ L of 300 μ M JW-1+2+p triplex containing 1.0 PNA equivalents was annealed with 25 mM HEPES, pH 7.0 for Crystallization Plate A. Because no successful crystallization work had ever been reported on these JW sequences, optimal crystallization conditions would have to be narrowed down from a general buffer set (Appendix K). For this plate, variables included pH (6.0, 6.5, 7.0, 7.5), PEG molecular weight (4000 or 8000), and PEG percentage (25%, 30%, 35%). Reservoir volume was held constant at 1 mL, and the droplet composition was 1 μ L triplex solution and 1 μ L well buffer. No precipitation was noted initially after plating. However, after three days, precipitation had occurred in all wells except 1, 7, 13, and 16, which remained as clear drops. While all 4 wells contained 25% PEG, three different pHs and both PEG molecular weights were represented, indicating that perhaps PEG concentration was the most important of the variables for the JW sequences. However, other wells containing 25% PEG (i.e. wells 4, 10, and 22) on Plate A had precipitated, suggesting that PEG percentage alone does not dictate whether a solution will precipitate or crystallize. After 2.5 months, wells 1, 7, 13, and 16 had also precipitated without producing any microcrystals.

Using the exact same general set of reservoir buffers used in plate A, a second crystallization experiment (Plate B) was set up using the JW-1+4+p triplex (Appendix L).

Once again, 40 μ L of 300 μ M sample containing 1.0 PNA equivalents was annealed with 25 mM HEPES, pH 7.0, and reservoir and droplet conditions were identical to plate A. Similar to Plate A, the samples showed no precipitation immediately after plating, but within three days, the majority had precipitated out of solution. Among those remaining as clear drops were wells 1, 4, 7, 10, 13, 16, 19, and 22 – representing a definite pattern of results. The reservoir buffer of each of these wells contained 25% PEG, with PEG molecular weight and pH once again varying. Unlike Plate A, every well containing a 25% PEG concentration remained clear even after several months had passed. In fact, roughly eight months after plating, well 1 (25% PEG 4000, pH 6.0) and well 10 (25% PEG 8000, pH 6.5) contained the largest and most defined crystalline formations observed on any plate. Unfortunately, at less than 0.2 mm, the crystals were not large enough to be analyzed by x-ray crystallography, but their existence holds promise for future crystallization efforts, and suggests the significance of 25% PEG concentration in the crystallization of JW sequences.

Looking collectively at the crystallization data from both the JT and JW strands, two things are readily apparent about research in this area of Janus Wedge triplexes: 1.) failures will always outweigh successes, and 2.) an ordered and systematic approach is essential if a three-dimensional structure is to be discovered. Without a doubt, the most promising results were contained in wells 1 and 10 of Plate B, but it was necessary to find a way to increase the crystal size in order for x-ray analysis to be possible. Subsequently, attempts were made to repeat this experiment using a more supersaturated solution. With more JW triplex in solution, it was hoped that there would be larger crystals forming out of solution. 40 μ L of 350 μ M JW-1+4+p triplex with 1.0 PNA equivalents was dried under high vacuum, and then annealed with 25 mM HEPES, pH 7.0. Addition of

annealing buffer, however, caused a large amount of the DNA to precipitate immediately. An additional 2.0 μL of annealing buffer along with 4.6 μL of 10 mM spermidine were added to dilute the complex to 300 μM . After filtering through a 0.22 μm Ultrafree-MC centrifugal filter at 10,000 rpm to eliminate residual triplex precipitates, sample was loaded onto a non-denaturing gel, which showed only faint laddering. Therefore, while increasing the complex concentration does increase the amount of triplex formed, it does so at the expense of the amount of triplex *in solution*. Because crystallization requires a supersaturated *solution*, increasing complex concentration beyond 300 μM does not appear to be a feasible means of increasing crystal size.

Other methods of growing larger crystals are possible and must be explored in a systemized manner. For example, altering buffer composition may improve the solubility of the JW triplex, allowing for higher complex concentrations. In future experiments, previous crystallization efforts would be repeated using 10 mM spermine, which has 4 positive charges per molecule, in the annealing buffer to possibly provide this added complex stability compared to spermidine, which has 3 positive charges. Additionally, if complex concentration cannot be stably increased above 300 μM , crystal growth can be improved through seeding experiments. Seeding involves taking a small amount of a microcrystal-containing droplet, such as those in wells 1 and 10 of Plate B, and forming a new droplet with buffer containing more triplex in solution. The seed crystal provides a template upon which the complex-containing solution may further crystallize. Typically, the degree of supersaturation required for seed formation is greater than that required for growth onto an existing crystal so complex concentration could be maintained at the 300 μM level.

Drew and Dickerson Dodecamer: Unlike Janus Wedge triplexes, three-dimensional structures of complexes known as Drew and Dickerson dodecamers have been well-documented. Pioneered in the early 1980s by Drew and Dickerson at the California Institute of Technology, dodecamers have a d(CGCGAATTCGCG) sequence and form self-complementary duplexes which form β -form helices. Dickerson and Drew have obtained highly detailed data obtained by x-ray crystallography to 1.9 Å resolution of these duplexes.¹⁹ Their data reveals the interlocking of the minor grooves of neighboring molecules, the amount of bend in the helical axis, the base pairs per turn, and the mean propeller twist.

Research by Loren D. Williams at the George Institute of Technology has provided even more detailed information about the interaction between β -form dodecamer duplexes and other molecular species.²⁰ Crystallization of the Drew and Dickerson sequence to 2.5 Å resolution revealed that within the A-T tract of the duplex, a spine of hydration partially composed of sodium ions is linked to a secondary spine of hydration. Furthermore, their diffraction patterns reveal a fully hydrated magnesium ion located in the major groove, suspected of interacting with cytosine bases of the duplex, as well as a partially ordered spermine molecule.

High resolution crystallization has also been successful with modified Drew and Dickerson dodecamers. For example, Hossain *et al.* successfully crystallized a d(CGCGAATTmo⁴CGCG)₂ duplex, where mo⁴C is the modified base 2'-deoxy-N⁴-methoxycytidine, by hanging drop vapor diffusion at 4°C.²¹ Analysis of the three-dimensional structure showed that sequence modification does not disrupt β -form helix formation. Electron density maps also confirmed that the mo⁴C residue pairs with an opposite strand G with Watson-Crick type geometry. Crystallization buffer contained

28% (v/v) 2-methyl-2,4-pentanediol (MPD), 36 mM Mg acetate, 9 mM spermine tetrahydrochloride, and 20 mM sodium cacodylate, pH 7.0.

Research is currently proceeding on a modified Dickerson dodecamer sequence synthesized and purified by post-graduate student Zhenhua. The d(CGCGAATTC*GCG) sequence contains a 2-amino-pyrimidine modified base at the C* residue. Crystallization efforts have been initiated using Hossain's work with a mo^4C modified base as a guide to crystallization. Dodecamer solutions have been annealed with 36 mM Mg acetate, 9 mM spermine tetrahydrochloride, and 20 mM sodium cacodylate at pH 6.6, 6.8, 7.0, and 7.2. Because of the high concentration of the pure dodecamer solution (603.56 μM), gel loading was done with only 0.10 μL of sample solution + 9.9 μL loading buffer (annealing buffer plus 30% glycerol). Visualization of the gel revealed no bands at all, which was reasonably interpreted as a consequence of the extremely small volume which was loaded. Even with a 2.5 μL pipet, 0.10 μL is at the lower extreme of its pipeting capacity, and it was surmised that accurate pipeting was not occurring. A follow-up gel will be run in which a larger volume of sample solution, which can be pipetted with certainty such as 0.5 μL , will be diluted to 2.5 μL with loading buffer. A 10 μL aliquot of this solution will have the same complex concentration as the solution loaded into the previous gel, but in this case, dilution will help overcome the limitations of the scientific equipment. As soon as Dodecamer duplex formation is confirmed by gel electrophoresis, a crystallization plate will be set up which has been designed based on the growing conditions of the Hossain crystal. Reservoir buffers of all 24 wells will contain 20 mM sodium cacodylate, 36 mM Mg acetate, and 9 mM spermine tetrahydrochloride. Samples will be either pH 6.6, 6.8, 7.0, or 7.2, and for each of the four pHs, MPD concentration

will be 20%, 22.5%, 25%, 26.5%, 28%, or 30% – consequently, each well will contain a unique buffer similar to the buffer used to crystallize the mo⁴C modified dodecamer.

Acknowledgments

I would like to sincerely thank Professor Larry McLaughlin, Meena, and the entire McLaughlin group for their support, patience, and guidance. At some point and in some way, every member of the group has contributed to the work presented here. I would also like to thank my family who, despite the physical distance, is with me always.

Appendices

Appendix A: The Assembly Steps of Solid-Phase DNA Synthesis

Appendix B: Table of Extinction Coefficients

Appendix C: Synthesized Strands

Appendix D: JT-2+3+p Plate 1 Reservoir Buffers

Appendix E: JT-2+3+p Plate 2 Reservoir Buffers

Appendix F: JT-2+3+p Plate 3 Reservoir Buffers

Appendix G: JT-2+3+p Plate 4 Reservoir Buffers

Appendix H: JT-2+3+p Plate 5 Reservoir Buffers

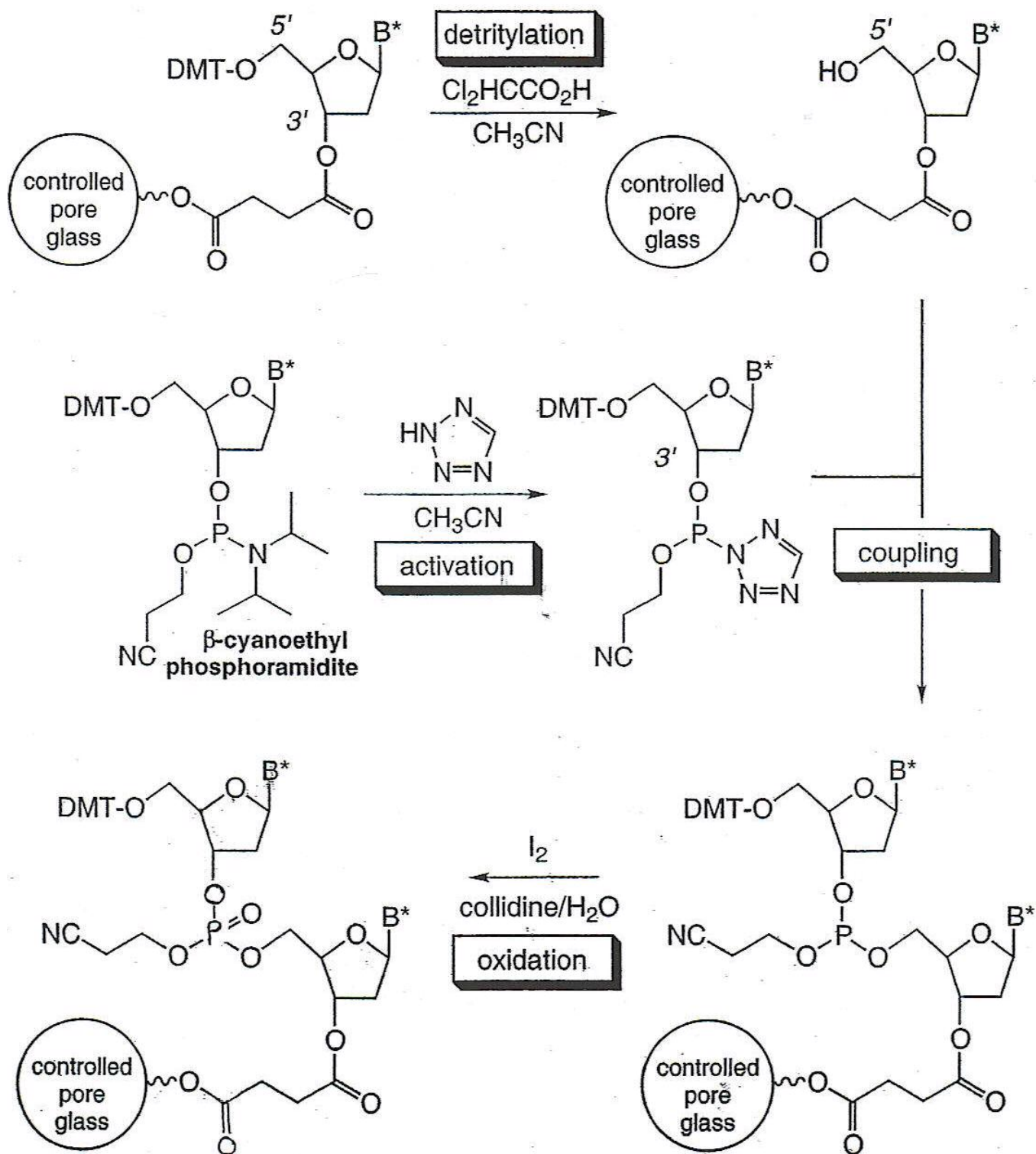
Appendix I: JT-2+3+p Plate 6 Reservoir Buffers

Appendix J: JT-2+3+p Plate 7 Reservoir Buffers

Appendix K: JW-1+2+p Plate A Reservoir Buffers

Appendix L: JW-1+4+p Plate B Reservoir Buffers

Appendix A: The Assembly Steps of Solid-Phase DNA Synthesis



Appendix B: Extinction Coefficients

Sample	Extinction Coefficient (cm ⁻¹ M ⁻¹)
G	11,500
T	8,700
C	7,400
A	15,400
2APy	1,500
JW-1	299,300
JW-2	287,300
JW-3	341,000
JW-4	280,700
JT-2	290,500
JT-3	271,900
M1-219	71,000

Appendix C: Synthesized Strands

Strand Name	Sequence
JT-2	5' – GCA CCG ACG CGT TTT TTT TCC GCG GCA GCC – 3'
JT-3	3' – CGT GGC TGC GCC CCC CCC CGG CGC CGT CGG – 5'
JW-1	5' – T GCA CCG ACG CGT TTT TTT TCC GCG GCA GCC – 3'
JW-2	3' – CGT GGC TGC GCC CCC CCC CGG CGC CGT CGG A – 5'
JW-3	5' – A GCA CCG ACG CGT TTT TTT TCC GCG GCA GCC – 3'
JW-4	3' – CGT GGC TGC GCC CCC CCC CGG CGC CGT CGG T – 5'

Appendix D: Crystallization Plate 1

Well #	Reservoir Buffer
1	0.01 M Zn acetate, 0.2 M Amm acetate, 0.05 M Na cacodylate, 25% PEG 4000, pH 6.0
2	0.01 M Zn acetate, 0.2 M Amm acetate, 0.05 M Na cacodylate, 30% PEG 4000, pH 6.0
3	0.01 M Zn acetate, 0.2 M Amm acetate, 0.05 M Na cacodylate, 35% PEG 4000, pH 6.0
4	0.01 M Zn acetate, 0.2 M Amm acetate, 0.05 M Na cacodylate, 25% PEG 8000, pH 6.0
5	0.01 M Zn acetate, 0.2 M Amm acetate, 0.05 M Na cacodylate, 30% PEG 8000, pH 6.0
6	0.01 M Zn acetate, 0.2 M Amm acetate, 0.05 M Na cacodylate, 35% PEG 8000, pH 6.0
7	0.01 M Zn acetate, 0.2 M Amm acetate, 0.05 M Na cacodylate, 25% PEG 4000, pH 6.5
8	0.01 M Zn acetate, 0.2 M Amm acetate, 0.05 M Na cacodylate, 30% PEG 4000, pH 6.5
9	0.01 M Zn acetate, 0.2 M Amm acetate, 0.05 M Na cacodylate, 35% PEG 4000, pH 6.5
10	0.01 M Zn acetate, 0.2 M Amm acetate, 0.05 M Na cacodylate, 25% PEG 8000, pH 6.5
11	0.01 M Zn acetate, 0.2 M Amm acetate, 0.05 M Na cacodylate, 30% PEG 8000, pH 6.5
12	0.01 M Zn acetate, 0.2 M Amm acetate, 0.05 M Na cacodylate, 35% PEG 8000, pH 6.5
13	0.01 M Zn acetate, 0.2 M Amm acetate, 0.05 M Na cacodylate, 25% PEG 4000, pH 7.0
14	0.01 M Zn acetate, 0.2 M Amm acetate, 0.05 M Na cacodylate, 30% PEG 4000, pH 7.0
15	0.01 M Zn acetate, 0.2 M Amm acetate, 0.05 M Na cacodylate, 35% PEG 4000, pH 7.0
16	0.01 M Zn acetate, 0.2 M Amm acetate, 0.05 M Na cacodylate, 25% PEG 8000, pH 7.0
17	0.01 M Zn acetate, 0.2 M Amm acetate, 0.05 M Na cacodylate, 30% PEG 8000, pH 7.0
18	0.01 M Zn acetate, 0.2 M Amm acetate, 0.05 M Na cacodylate, 35% PEG 8000, pH 7.0
19	0.01 M Zn acetate, 0.2 M Amm acetate, 0.05 M Na cacodylate, 25% PEG 4000, pH 7.5
20	0.01 M Zn acetate, 0.2 M Amm acetate, 0.05 M Na cacodylate, 30% PEG 4000, pH 7.5
21	0.01 M Zn acetate, 0.2 M Amm acetate, 0.05 M Na cacodylate, 35% PEG 4000, pH 7.5
22	0.01 M Zn acetate, 0.2 M Amm acetate, 0.05 M Na cacodylate, 25% PEG 8000, pH 7.5
23	0.01 M Zn acetate, 0.2 M Amm acetate, 0.05 M Na cacodylate, 30% PEG 8000, pH 7.5
24	0.01 M Zn acetate, 0.2 M Amm acetate, 0.05 M Na cacodylate, 35% PEG 8000, pH 7.5

Appendix E: Crystallization Plate 2

Well #	Conc (uM)	Buffer
1	200	0.01 M Zn acetate, 0.2 M Amm acetate, 0.05 M Na cacodylate, 32.5% PEG 8000
2	200	0.01 M Zn acetate, 0.2 M Amm acetate, 0.05 M Na cacodylate, 35% PEG 8000
3	200	0.01 M Zn acetate, 0.2 M Amm acetate, 0.05 M Na cacodylate, 37.5% PEG 8000
4	200	0.01 M Zn acetate, 0.2 M Amm acetate, 0.05 M Na cacodylate, 40% PEG 8000
5	200	0.01 M Zn acetate, 0.2 M Amm acetate, 0.05 M Na cacodylate, 42.5% PEG 8000
6	200	0.01 M Zn acetate, 0.2 M Amm acetate, 0.05 M Na cacodylate, 45% PEG 8000
7	225	0.01 M Zn acetate, 0.2 M Amm acetate, 0.05 M Na cacodylate, 32.5% PEG 8000
8	225	0.01 M Zn acetate, 0.2 M Amm acetate, 0.05 M Na cacodylate, 35% PEG 8000
9	225	0.01 M Zn acetate, 0.2 M Amm acetate, 0.05 M Na cacodylate, 37.5% PEG 8000
10	225	0.01 M Zn acetate, 0.2 M Amm acetate, 0.05 M Na cacodylate, 40% PEG 8000
11	225	0.01 M Zn acetate, 0.2 M Amm acetate, 0.05 M Na cacodylate, 42.5% PEG 8000
12	225	0.01 M Zn acetate, 0.2 M Amm acetate, 0.05 M Na cacodylate, 45% PEG 8000
13	250	0.01 M Zn acetate, 0.2 M Amm acetate, 0.05 M Na cacodylate, 32.5% PEG 8000
14	250	0.01 M Zn acetate, 0.2 M Amm acetate, 0.05 M Na cacodylate, 35% PEG 8000
15	250	0.01 M Zn acetate, 0.2 M Amm acetate, 0.05 M Na cacodylate, 37.5% PEG 8000
16	250	0.01 M Zn acetate, 0.2 M Amm acetate, 0.05 M Na cacodylate, 40% PEG 8000
17	250	0.01 M Zn acetate, 0.2 M Amm acetate, 0.05 M Na cacodylate, 42.5% PEG 8000
18	250	0.01 M Zn acetate, 0.2 M Amm acetate, 0.05 M Na cacodylate, 45% PEG 8000
19	300	0.01 M Zn acetate, 0.2 M Amm acetate, 0.05 M Na cacodylate, 32.5% PEG 8000
20	300	0.01 M Zn acetate, 0.2 M Amm acetate, 0.05 M Na cacodylate, 35% PEG 8000
21	300	0.01 M Zn acetate, 0.2 M Amm acetate, 0.05 M Na cacodylate, 37.5% PEG 8000
22	300	0.01 M Zn acetate, 0.2 M Amm acetate, 0.05 M Na cacodylate, 40% PEG 8000
23	300	0.01 M Zn acetate, 0.2 M Amm acetate, 0.05 M Na cacodylate, 42.5% PEG 8000
24	300	0.01 M Zn acetate, 0.2 M Amm acetate, 0.05 M Na cacodylate, 45% PEG 8000

Appendix F: Crystallization Plate 3

Well #	S:B Ratio	Res Vol	Buffer
1	1 + 1	1 mL	0.01 M Mg acetate, 0.2 M Amm acetate, 0.05 M Na cacodylate, pH 6.0, 30% PEG 4000
2	1 + 1	1 mL	0.01 M Mg acetate, 0.2 M Amm acetate, 0.05 M Na cacodylate, pH 6.5, 30% PEG 4000
3	1 + 1	1 mL	0.01 M Mg acetate, 0.2 M Amm acetate, 0.05 M Na cacodylate, pH 7.0, 30% PEG 4000
4	1 + 1	1 mL	0.01 M Mg acetate, 0.2 M Amm acetate, 0.05 M Na cacodylate, pH 7.0, 35% PEG 4000
5	1 + 1	1 mL	0.01 M Mg acetate, 0.2 M Amm acetate, 0.05 M Na cacodylate, pH 7.5, 30% PEG 4000
6	1 + 1	1 mL	0.01 M Mg acetate, 0.2 M Amm acetate, 0.05 M Na cacodylate, pH 7.5, 25% PEG 8000
7	2 + 1	1 mL	0.01 M Mg acetate, 0.2 M Amm acetate, 0.05 M Na cacodylate, pH 6.0, 30% PEG 4000
8	2 + 1	1 mL	0.01 M Mg acetate, 0.2 M Amm acetate, 0.05 M Na cacodylate, pH 6.5, 30% PEG 4000
9	2 + 1	1 mL	0.01 M Mg acetate, 0.2 M Amm acetate, 0.05 M Na cacodylate, pH 7.0, 30% PEG 4000
10	2 + 1	1 mL	0.01 M Mg acetate, 0.2 M Amm acetate, 0.05 M Na cacodylate, pH 7.0, 35% PEG 4000
11	2 + 1	1 mL	0.01 M Mg acetate, 0.2 M Amm acetate, 0.05 M Na cacodylate, pH 7.5, 30% PEG 4000
12	2 + 1	1 mL	0.01 M Mg acetate, 0.2 M Amm acetate, 0.05 M Na cacodylate, pH 7.5, 25% PEG 8000
13	1 + 1	0.5 mL	0.01 M Mg acetate, 0.2 M Amm acetate, 0.05 M Na cacodylate, pH 6.0, 30% PEG 4000
14	1 + 1	0.5 mL	0.01 M Mg acetate, 0.2 M Amm acetate, 0.05 M Na cacodylate, pH 6.5, 30% PEG 4000
15	1 + 1	0.5 mL	0.01 M Mg acetate, 0.2 M Amm acetate, 0.05 M Na cacodylate, pH 7.0, 30% PEG 4000
16	1 + 1	0.5 mL	0.01 M Mg acetate, 0.2 M Amm acetate, 0.05 M Na cacodylate, pH 7.0, 35% PEG 4000
17	1 + 1	0.5 mL	0.01 M Mg acetate, 0.2 M Amm acetate, 0.05 M Na cacodylate, pH 7.5, 30% PEG 4000
18	1 + 1	0.5 mL	0.01 M Mg acetate, 0.2 M Amm acetate, 0.05 M Na cacodylate, pH 7.5, 25% PEG 8000
19	2 + 1	0.5 mL	0.01 M Mg acetate, 0.2 M Amm acetate, 0.05 M Na cacodylate, pH 6.0, 30% PEG 4000
20	2 + 1	0.5 mL	0.01 M Mg acetate, 0.2 M Amm acetate, 0.05 M Na cacodylate, pH 6.5, 30% PEG 4000
21	2 + 1	0.5 mL	0.01 M Mg acetate, 0.2 M Amm acetate, 0.05 M Na cacodylate, pH 7.0, 30% PEG 4000
22	2 + 1	0.5 mL	0.01 M Mg acetate, 0.2 M Amm acetate, 0.05 M Na cacodylate, pH 7.0, 35% PEG 4000

Appendix G: Crystallization Plate 4

Well #	S:B Ratio	Res Vol	Buffer
1	1+ 1	1 mL	0.01 M Mg acetate, 0.2 M Amm acetate, 0.05 M Na cacodylate, pH 6.0, 30% PEG 10000
2	2 + 2	1 mL	0.01 M Mg acetate, 0.2 M Amm acetate, 0.05 M Na cacodylate, pH 6.0, 30% PEG 10000
3	1+ 1	0.5 mL	0.01 M Mg acetate, 0.2 M Amm acetate, 0.05 M Na cacodylate, pH 6.0, 30% PEG 10000
4	2 + 2	0.5 mL	0.01 M Mg acetate, 0.2 M Amm acetate, 0.05 M Na cacodylate, pH 6.0, 30% PEG 10000
7	1+ 1	1 mL	0.01 M Mg acetate, 0.2 M Amm acetate, 0.05 M Na cacodylate, pH 6.0, 35% PEG 8000
8	2 + 2	1 mL	0.01 M Mg acetate, 0.2 M Amm acetate, 0.05 M Na cacodylate, pH 6.0, 35% PEG 8000
9	1+ 1	0.5 mL	0.01 M Mg acetate, 0.2 M Amm acetate, 0.05 M Na cacodylate, pH 6.0, 35% PEG 8000
10	2 + 2	0.5 mL	0.01 M Mg acetate, 0.2 M Amm acetate, 0.05 M Na cacodylate, pH 6.0, 35% PEG 8000
13	1+ 1	1 mL	0.01 M Mg acetate, 0.2 M Amm acetate, 0.05 M Na cacodylate, pH 6.5, 25% PEG 10000
14	2 + 2	1 mL	0.01 M Mg acetate, 0.2 M Amm acetate, 0.05 M Na cacodylate, pH 6.5, 25% PEG 10000
15	1+ 1	0.5 mL	0.01 M Mg acetate, 0.2 M Amm acetate, 0.05 M Na cacodylate, pH 6.5, 25% PEG 10000
16	2 + 2	0.5 mL	0.01 M Mg acetate, 0.2 M Amm acetate, 0.05 M Na cacodylate, pH 6.5, 25% PEG 10000
19	1+ 1	1 mL	0.01 M Mg acetate, 0.2 M Amm acetate, 0.05 M Na cacodylate, pH 6.5, 30% PEG 8000
20	2 + 2	1 mL	0.01 M Mg acetate, 0.2 M Amm acetate, 0.05 M Na cacodylate, pH 6.5, 30% PEG 8000
21	1+ 1	0.5 mL	0.01 M Mg acetate, 0.2 M Amm acetate, 0.05 M Na cacodylate, pH 6.5, 30% PEG 8000
22	2 + 2	0.5 mL	0.01 M Mg acetate, 0.2 M Amm acetate, 0.05 M Na cacodylate, pH 6.5, 30% PEG 8000

Appendix H: Crystallization Plate 5

Well #	S:B Ratio	Buffer
1	1 + 1	0.01 M Zn acetate, 0.2 M Amm acetate, 0.05 M Na cacodylate, 30% PEG 8000, pH 6.0
2	2 + 1	0.01 M Zn acetate, 0.2 M Amm acetate, 0.05 M Na cacodylate, 30% PEG 8000, pH 6.0
3	2 + 2	0.01 M Zn acetate, 0.2 M Amm acetate, 0.05 M Na cacodylate, 30% PEG 8000, pH 6.0
7	1 + 1	0.01 M Zn acetate, 0.2 M Amm acetate, 0.05 M Na cacodylate, 30% PEG 8000, pH 6.5
8	2 + 1	0.01 M Zn acetate, 0.2 M Amm acetate, 0.05 M Na cacodylate, 30% PEG 8000, pH 6.5
9	2 + 2	0.01 M Zn acetate, 0.2 M Amm acetate, 0.05 M Na cacodylate, 30% PEG 8000, pH 6.5
13	1 + 1	0.01 M Zn acetate, 0.2 M Amm acetate, 0.05 M Na cacodylate, 30% PEG 8000, pH 7.0
14	2 + 1	0.01 M Zn acetate, 0.2 M Amm acetate, 0.05 M Na cacodylate, 30% PEG 8000, pH 7.0
15	2 + 2	0.01 M Zn acetate, 0.2 M Amm acetate, 0.05 M Na cacodylate, 30% PEG 8000, pH 7.0
19	1 + 1	0.01 M Zn acetate, 0.2 M Amm acetate, 0.05 M Na cacodylate, 30% PEG 8000, pH 7.5
20	2 + 1	0.01 M Zn acetate, 0.2 M Amm acetate, 0.05 M Na cacodylate, 30% PEG 8000, pH 7.5
21	2 + 2	0.01 M Zn acetate, 0.2 M Amm acetate, 0.05 M Na cacodylate, 30% PEG 8000, pH 7.5
22	1 + 1	0.01 M Zn acetate, 0.2 M Amm acetate, 0.05 M Na cacodylate, 30% PEG 8000, pH 7.5
23	2 + 2	0.01 M Zn acetate, 0.2 M Amm acetate, 0.05 M Na cacodylate, 30% PEG 8000, pH 7.5

Appendix I: Crystallization Plate 6

Well #	Buffer
1	0.01 M Zn acetate, 0.2 M Amm acetate, 0.05 M Na cacodylate, 20% PEG 10000, pH 6.5
2	0.01 M Zn acetate, 0.2 M Amm acetate, 0.05 M Na cacodylate, 20% PEG 10000, pH 7.0
3	0.01 M Zn acetate, 0.2 M Amm acetate, 0.05 M Na cacodylate, 20% PEG 10000, pH 7.5
4	0.01 M Mg acetate, 0.2 M Amm acetate, 0.05 M Na cacodylate, 20% PEG 10000, pH 6.5
5	0.01 M Mg acetate, 0.2 M Amm acetate, 0.05 M Na cacodylate, 20% PEG 10000, pH 7.0
6	0.01 M Mg acetate, 0.2 M Amm acetate, 0.05 M Na cacodylate, 20% PEG 10000, pH 7.5
7	0.01 M Zn acetate, 0.2 M Amm acetate, 0.05 M Na cacodylate, 25% PEG 10000, pH 6.5
8	0.01 M Zn acetate, 0.2 M Amm acetate, 0.05 M Na cacodylate, 25% PEG 10000, pH 7.0
9	0.01 M Zn acetate, 0.2 M Amm acetate, 0.05 M Na cacodylate, 25% PEG 10000, pH 7.5
10	0.01 M Mg acetate, 0.2 M Amm acetate, 0.05 M Na cacodylate, 25% PEG 10000, pH 6.5
11	0.01 M Mg acetate, 0.2 M Amm acetate, 0.05 M Na cacodylate, 25% PEG 10000, pH 7.0
12	0.01 M Mg acetate, 0.2 M Amm acetate, 0.05 M Na cacodylate, 25% PEG 10000, pH 7.5
13	0.01 M Zn acetate, 0.2 M Amm acetate, 0.05 M Na cacodylate, 30% PEG 10000, pH 6.5
14	0.01 M Zn acetate, 0.2 M Amm acetate, 0.05 M Na cacodylate, 30% PEG 10000, pH 7.0
15	0.01 M Zn acetate, 0.2 M Amm acetate, 0.05 M Na cacodylate, 30% PEG 10000, pH 7.5
16	0.01 M Mg acetate, 0.2 M Amm acetate, 0.05 M Na cacodylate, 30% PEG 10000, pH 6.5
17	0.01 M Mg acetate, 0.2 M Amm acetate, 0.05 M Na cacodylate, 30% PEG 10000, pH 7.0
18	0.01 M Mg acetate, 0.2 M Amm acetate, 0.05 M Na cacodylate, 30% PEG 10000, pH 7.5
19	0.01 M Zn acetate, 0.2 M Amm acetate, 0.05 M Na cacodylate, 35% PEG 10000, pH 6.5
20	0.01 M Zn acetate, 0.2 M Amm acetate, 0.05 M Na cacodylate, 35% PEG 10000, pH 7.0
21	0.01 M Zn acetate, 0.2 M Amm acetate, 0.05 M Na cacodylate, 35% PEG 10000, pH 7.5
22	0.01 M Mg acetate, 0.2 M Amm acetate, 0.05 M Na cacodylate, 35% PEG 10000, pH 6.5
23	0.01 M Mg acetate, 0.2 M Amm acetate, 0.05 M Na cacodylate, 35% PEG 10000, pH 7.0
24	0.01 M Mg acetate, 0.2 M Amm acetate, 0.05 M Na cacodylate, 35% PEG 10000, pH 7.5

Appendix J: Crystallization Plate 7

Well #	Buffer
1	0.01 M Mg acetate, 0.2 M Amm acetate, 0.05 M Na cacodylate, 35% PEG 8000, pH 6.0
2	0.01 M Mg acetate, 0.2 M Amm acetate, 0.05 M Na cacodylate, 35% PEG 8000, pH 6.0
3	0.01 M Mg acetate, 0.2 M Amm acetate, 0.05 M Na cacodylate, 35% PEG 8000, pH 6.0
4	0.01 M Mg acetate, 0.2 M Amm acetate, 0.05 M Na cacodylate, 35% PEG 8000, pH 6.0
5	0.01 M Mg acetate, 0.2 M Amm acetate, 0.05 M Na cacodylate, 35% PEG 8000, pH 6.0
6	0.01 M Mg acetate, 0.2 M Amm acetate, 0.05 M Na cacodylate, 35% PEG 8000, pH 6.0
7	0.01 M Mg acetate, 0.2 M Amm acetate, 0.05 M Na cacodylate, 35% PEG 8000, pH 6.0
8	0.01 M Mg acetate, 0.2 M Amm acetate, 0.05 M Na cacodylate, 35% PEG 8000, pH 6.0
9	0.01 M Mg acetate, 0.2 M Amm acetate, 0.05 M Na cacodylate, 35% PEG 8000, pH 6.0
10	0.01 M Mg acetate, 0.2 M Amm acetate, 0.05 M Na cacodylate, 35% PEG 8000, pH 6.0
11	0.01 M Mg acetate, 0.2 M Amm acetate, 0.05 M Na cacodylate, 35% PEG 8000, pH 6.0
12	0.01 M Mg acetate, 0.2 M Amm acetate, 0.05 M Na cacodylate, 35% PEG 8000, pH 6.0
13	0.01 M Mg acetate, 0.2 M Amm acetate, 0.05 M Na cacodylate, 25% PEG 4000, pH 6.5
14	0.01 M Mg acetate, 0.2 M Amm acetate, 0.05 M Na cacodylate, 25% PEG 4000, pH 6.5
15	0.01 M Mg acetate, 0.2 M Amm acetate, 0.05 M Na cacodylate, 25% PEG 4000, pH 6.5
16	0.01 M Mg acetate, 0.2 M Amm acetate, 0.05 M Na cacodylate, 25% PEG 4000, pH 6.5
17	0.01 M Mg acetate, 0.2 M Amm acetate, 0.05 M Na cacodylate, 25% PEG 4000, pH 6.5
18	0.01 M Mg acetate, 0.2 M Amm acetate, 0.05 M Na cacodylate, 25% PEG 4000, pH 6.5
19	0.01 M Mg acetate, 0.2 M Amm acetate, 0.05 M Na cacodylate, 25% PEG 4000, pH 6.5
20	0.01 M Mg acetate, 0.2 M Amm acetate, 0.05 M Na cacodylate, 25% PEG 4000, pH 6.5
21	0.01 M Mg acetate, 0.2 M Amm acetate, 0.05 M Na cacodylate, 25% PEG 4000, pH 6.5
22	0.01 M Mg acetate, 0.2 M Amm acetate, 0.05 M Na cacodylate, 25% PEG 4000, pH 6.5
23	0.01 M Mg acetate, 0.2 M Amm acetate, 0.05 M Na cacodylate, 25% PEG 4000, pH 6.5
24	0.01 M Mg acetate, 0.2 M Amm acetate, 0.05 M Na cacodylate, 25% PEG 4000, pH 6.5

Appendix K: Crystallization Plate A

Well #	Buffer
1	0.01 M Mg acetate, 0.2 M Amm acetate, 0.05 M Na cacodylate, 25% PEG 4000, pH 6.0
2	0.01 M Mg acetate, 0.2 M Amm acetate, 0.05 M Na cacodylate, 30% PEG 4000, pH 6.0
3	0.01 M Mg acetate, 0.2 M Amm acetate, 0.05 M Na cacodylate, 35% PEG 4000, pH 6.0
4	0.01 M Mg acetate, 0.2 M Amm acetate, 0.05 M Na cacodylate, 25% PEG 8000, pH 6.0
5	0.01 M Mg acetate, 0.2 M Amm acetate, 0.05 M Na cacodylate, 30% PEG 8000, pH 6.0
6	0.01 M Mg acetate, 0.2 M Amm acetate, 0.05 M Na cacodylate, 35% PEG 8000, pH 6.0
7	0.01 M Mg acetate, 0.2 M Amm acetate, 0.05 M Na cacodylate, 25% PEG 4000, pH 6.5
8	0.01 M Mg acetate, 0.2 M Amm acetate, 0.05 M Na cacodylate, 30% PEG 4000, pH 6.5
9	0.01 M Mg acetate, 0.2 M Amm acetate, 0.05 M Na cacodylate, 35% PEG 4000, pH 6.5
10	0.01 M Mg acetate, 0.2 M Amm acetate, 0.05 M Na cacodylate, 25% PEG 8000, pH 6.5
11	0.01 M Mg acetate, 0.2 M Amm acetate, 0.05 M Na cacodylate, 30% PEG 8000, pH 6.5
12	0.01 M Mg acetate, 0.2 M Amm acetate, 0.05 M Na cacodylate, 35% PEG 8000, pH 6.5
13	0.01 M Mg acetate, 0.2 M Amm acetate, 0.05 M Na cacodylate, 25% PEG 4000, pH 7.0
14	0.01 M Mg acetate, 0.2 M Amm acetate, 0.05 M Na cacodylate, 30% PEG 4000, pH 7.0
15	0.01 M Mg acetate, 0.2 M Amm acetate, 0.05 M Na cacodylate, 35% PEG 4000, pH 7.0
16	0.01 M Mg acetate, 0.2 M Amm acetate, 0.05 M Na cacodylate, 25% PEG 8000, pH 7.0
17	0.01 M Mg acetate, 0.2 M Amm acetate, 0.05 M Na cacodylate, 30% PEG 8000, pH 7.0
18	0.01 M Mg acetate, 0.2 M Amm acetate, 0.05 M Na cacodylate, 35% PEG 8000, pH 7.0
19	0.01 M Mg acetate, 0.2 M Amm acetate, 0.05 M Na cacodylate, 25% PEG 4000, pH 7.5
20	0.01 M Mg acetate, 0.2 M Amm acetate, 0.05 M Na cacodylate, 30% PEG 4000, pH 7.5
21	0.01 M Mg acetate, 0.2 M Amm acetate, 0.05 M Na cacodylate, 35% PEG 4000, pH 7.5
22	0.01 M Mg acetate, 0.2 M Amm acetate, 0.05 M Na cacodylate, 25% PEG 8000, pH 7.5
23	0.01 M Mg acetate, 0.2 M Amm acetate, 0.05 M Na cacodylate, 30% PEG 8000, pH 7.5
24	0.01 M Mg acetate, 0.2 M Amm acetate, 0.05 M Na cacodylate, 35% PEG 8000, pH 7.5

Appendix L: Crystallization Plate B

Well #	Buffer
1	0.01 M Mg acetate, 0.2 M Amm acetate, 0.05 M Na cacodylate, 25% PEG 4000, pH 6.0
2	0.01 M Mg acetate, 0.2 M Amm acetate, 0.05 M Na cacodylate, 30% PEG 4000, pH 6.0
3	0.01 M Mg acetate, 0.2 M Amm acetate, 0.05 M Na cacodylate, 35% PEG 4000, pH 6.0
4	0.01 M Mg acetate, 0.2 M Amm acetate, 0.05 M Na cacodylate, 25% PEG 8000, pH 6.0
5	0.01 M Mg acetate, 0.2 M Amm acetate, 0.05 M Na cacodylate, 30% PEG 8000, pH 6.0
6	0.01 M Mg acetate, 0.2 M Amm acetate, 0.05 M Na cacodylate, 35% PEG 8000, pH 6.0
7	0.01 M Mg acetate, 0.2 M Amm acetate, 0.05 M Na cacodylate, 25% PEG 4000, pH 6.5
8	0.01 M Mg acetate, 0.2 M Amm acetate, 0.05 M Na cacodylate, 30% PEG 4000, pH 6.5
9	0.01 M Mg acetate, 0.2 M Amm acetate, 0.05 M Na cacodylate, 35% PEG 4000, pH 6.5
10	0.01 M Mg acetate, 0.2 M Amm acetate, 0.05 M Na cacodylate, 25% PEG 8000, pH 6.5
11	0.01 M Mg acetate, 0.2 M Amm acetate, 0.05 M Na cacodylate, 30% PEG 8000, pH 6.5
12	0.01 M Mg acetate, 0.2 M Amm acetate, 0.05 M Na cacodylate, 35% PEG 8000, pH 6.5
13	0.01 M Mg acetate, 0.2 M Amm acetate, 0.05 M Na cacodylate, 25% PEG 4000, pH 7.0
14	0.01 M Mg acetate, 0.2 M Amm acetate, 0.05 M Na cacodylate, 30% PEG 4000, pH 7.0
15	0.01 M Mg acetate, 0.2 M Amm acetate, 0.05 M Na cacodylate, 35% PEG 4000, pH 7.0
16	0.01 M Mg acetate, 0.2 M Amm acetate, 0.05 M Na cacodylate, 25% PEG 8000, pH 7.0
17	0.01 M Mg acetate, 0.2 M Amm acetate, 0.05 M Na cacodylate, 30% PEG 8000, pH 7.0
18	0.01 M Mg acetate, 0.2 M Amm acetate, 0.05 M Na cacodylate, 35% PEG 8000, pH 7.0
19	0.01 M Mg acetate, 0.2 M Amm acetate, 0.05 M Na cacodylate, 25% PEG 4000, pH 7.5
20	0.01 M Mg acetate, 0.2 M Amm acetate, 0.05 M Na cacodylate, 30% PEG 4000, pH 7.5
21	0.01 M Mg acetate, 0.2 M Amm acetate, 0.05 M Na cacodylate, 35% PEG 4000, pH 7.5
22	0.01 M Mg acetate, 0.2 M Amm acetate, 0.05 M Na cacodylate, 25% PEG 8000, pH 7.5
23	0.01 M Mg acetate, 0.2 M Amm acetate, 0.05 M Na cacodylate, 30% PEG 8000, pH 7.5
24	0.01 M Mg acetate, 0.2 M Amm acetate, 0.05 M Na cacodylate, 35% PEG 8000, pH 7.5

-
- ¹ Felsenfeld, F., Davies, A. G. & Rich, A. (1957). Formation of the three-stranded polynucleotide molecule. *J. Am. Chem. Soc.* 79, 2023-2024.
- ² Lee, J. S., Johnson, D. A. & Morgan, A. R. (1979). Complexes formed by (pyrimidine)_n • (purine)_n DNAs on lowering the pH are three-stranded. *Nucleic Acids Res.* 6, 3073-3091.
- ³ Lee, J. S., Woodsworth, M. L., Latimer, L. J. & Morgan, A. R. (1984). Poly(pyrimidine)•poly(purine) synthetic DNAs containing 5-methylcytosine form stable triplexes at neutral pH. *Nucleic Acids Res.* 12, 6603-6614.
- ⁴ Figures obtained from Fox Lab, Department of Biology and Biochemistry, University of Houston.
- ⁵ Moser, H. E. & Dervan, P. B. (1987). Sequence-specific cleavage of double helical DNA by triple helix formation. *Science* 238, 645-650.
- ⁶ Cooney, M., Czernuszewicz, G., Postel, E. H., Flint, S. J., & Hogan, M. E. (1988). Site specific oligonucleotide binding represses transcription of the human c-myc gene in vitro. *Science* 241, 456-459.
- ⁷ Figure obtained from Eurogentec.
- ⁸ Figure obtained from Eurogentec.
- ⁹ Branda, N., Kurz, G., Lehn, J. M. (1996). JANUS WEDGES: a new approach towards nucleobase-pair recognition. *Chem. Commun.* 21, 2443-2444.
- ¹⁰ Figure obtained from Larry McLaughlin.
- ¹¹ Chen, D., Meena, M., Sharma, S., & McLaughlin, L. W. (2004). Formation and Stability of a Janus-Wedge Type of DNA Triplex. *J. Am. Chem. Soc.* 126, 70-71.
- ¹² Figure obtained from Larry McLaughlin.
- ¹³ Rasmussen, H., & Sandholm, J. (1997). Crystal structure of a peptide nucleic acid (PNA) duplex at 1.7 Å resolution. *Nature Struct. Bio.* 4, 98-101.
- ¹⁴ Kastrup, J. S., Pilgaard, M., Jorgensen, F. S., Nielson, P. E., & Rasmussen, H. (1995). Crystallization and preliminary X-ray analysis of a PNA-DNA complex. *Fed. Of European Biochem. Soc.* 363, 115-117.
- ¹⁵ Betts, L., Josey, J. A., Veal, J. M., & Jordan, S. R. (1995). A nucleic acid triple helix formed by a peptide nucleic acid-DNA complex. *Science.* 270, 1838-1841.
- ¹⁶ Figure courtesy of Professor Marc Snapper, Boston College Chemistry Department
- ¹⁷ Description and figures provided by post-doctorate researcher Meena.
- ¹⁸ Hampel, A., Labananskas, M., Connors, P. G., Kirkegard, L., RajBhandary, U. L., & Sigler, P. B. (1968). Single crystals of transfer RNA from formylmethionine and phenylalanine transfer RNA's. *Science* 162, 1384.
- ¹⁹ Drew, H. R., Wing, R. M., Takano, T., Broka, C., Tanaka, S., Itakura, K., & Dickerson, R. E. (1981). Structure of a B-DNA dodecamer: conformation and dynamics. *Proc. Natl. Acad. Sci.* 78, 2179-2183.
- ²⁰ Shui, X., McFail-Isom, L, Hu, G. G., & Williams, L. D. (1998). The B-DNA Dodecamer at High Resolution Reveals a Spine of Water on Sodium. *Biochem.* 37, 8341-8355.
- ²¹ Hossain, M. T., Chatake, T., Hikima, T., Tsunoda, M., Sunami, T., Ueno, Y., Matsuda, A., & Takenaka, A. (2001). Crystallographic Studies on Damaged DNAs: III. N⁴-Methoxycytosine Can Form Both Watson-Crick Type and Wobbled Base Pairs in a β-Form Duplex. *J. Biochem.* 130, 9-12.